AXL is an Essential Factor and Therapeutic Target for Metastatic Ovarian Cancer

Erinn B. Rankin[1], **Katherine C. Fuh**[1,2], **Tiffany E. Taylor**[1], **Adam J. Krieg**[1], **Margaret Musser**[3], **Jenny Yuan**[4], **Kevin Wei**[4], **Calvin J. Kuo**[4], **Teri A. Longacre**[5], and **Amato J. Giaccia**[1]

[1]Division of Radiation and Cancer Biology, Department of Radiation Oncology, Center for Clinical Sciences Research, Department of Radiation Oncology, University, Stanford, California 94303-5152

[2]Division of Gynecologic Oncology, Department of Radiation Oncology, University, Stanford, California 94303-5152

[4]Division of Hematology, Department of Radiation Oncology, University, Stanford, California 94303-5152

[5]Department of Pathology Stanford University, Stanford, California 94303-5152;

[3]College of Veterinary Medicine, University of Illinois

Abstract

The receptor tyrosine kinase AXL is thought to play a role in metastasis, but the therapeutic efficacy of an AXL targeting agent remains largely untested in metastatic disease. In this study, we defined AXL as a therapeutic target for metastatic ovarian cancer. AXL is primarily expressed in metastases and advanced stage human ovarian tumors but not in normal ovarian epithelium. Genetic inhibition of AXL in human metastatic ovarian tumor cells is sufficient to prevent the initiation of metastatic disease in vivo. Mechanistically, inhibition of AXL signaling in animals with metastatic disease results in decreased invasion and MMP activity. Most importantly, soluble human AXL receptors that imposed a specific blockade of the GAS6/AXL pathway had a profound inhibitory effect on progression of established metastatic ovarian cancer without normal tissue toxicity. These results offer the first genetic validation of GAS6/AXL targeting as an effective strategy for inhibition of metastatic tumor progression in vivo. Furthermore, this study defines soluble AXL receptor therapy as a therapeutic candidate agent treating metastatic ovarian cancer, where current therapies are ineffective.

Keywords

matrix metalloproteinase; epithelial ovarian cancer; metastasis; growth arrest specific gene 6

Introduction

Epithelial ovarian cancer (EOC) is a devastating disease that affects 1/72 women in the United States. It is the 4th leading cause of cancer related deaths among women in the United States and is the primary cause of all gynecologic cancer-related deaths worldwide. Approximately 70% of patients diagnosed with EOC present with stage III or IV disease in

which the tumor has disseminated beyond the ovaries and pelvic organs to the peritoneum and mesothelial lining of abdominal organs including the diaphragm, stomach, omentum, liver, and intestines. Despite current surgical and cytotoxic therapies, 80% of patients diagnosed with advanced EOC develop recurrent disease and only 30% of patients survive 5 years following diagnosis (1). These findings underscore that tumor metastasis remains a major clinical challenge in the treatment of EOC. Thus, the identification of molecular targets regulating ovarian metastasis is critical for the development of more effective therapeutic agents for the treatment of EOC.

Ovarian tumor metastasis is a multistep process that is influenced by cell intrinsic factors, the tissue microenvironment, and immune activity (2, 3). The demonstration of premetastatic niches that can direct metastatic tumor cell behavior and the reseeding of primary tumors by circulating tumor cells has reinforced the importance of the dynamic relationship between the primary tumor and its metastatic derivatives (4). The interplay of these factors has been proposed to explain why to date there has not been successful targeting of metastatic disease. Intrinsic cellular activities associated with the metastatic cascade include invasion/migration, changes in cellular adhesion, survival, and proliferation (5). Invasion and migration are particularly important for metastatic ovarian tumor cells as these processes are involved in both early and late stages of metastasis and are found to be specifically upregulated in high-grade tumors and metastases (6, 7). Therefore, the development of therapeutic agents targeting invasion/migration may be a useful strategy to inhibit metastasis and may provide clinical benefits to patients with advanced ovarian cancer.

The receptor tyrosine kinase AXL has recently been identified as a critical factor driving tumor cell invasion and migration. AXL is the founding member of the TAM family of RTKs, which include Tyro3 (or SKY), AXL, and MER (8, 9). TAM receptors are characterized by an extracellular domain containing two immunoglobulin-like (IG) domains and two fibronectin type 3-like domains. The ligand GAS6 (growth arrest specific gene-6) is the common ligand for all three receptors. GAS6 has highest affinity for AXL and is the only known ligand for AXL (10). GAS6 binding to AXL results in AXL dimerization and autophosphorylation of tyrosine residues 779, 821, and 866 which serve as docking sites for a variety of intracellular signaling molecules (11). AXL signaling has been shown to promote cellular adhesion, invasion, migration, proinflammatory cytokine production, anti-apoptosis, proliferation, and survival (11).

In tumor cells, AXL plays an important role in regulating cellular invasion and migration. Overexpression of AXL in tumor cells with low metastatic potential promotes migration and invasion (12–14). In addition, blockade of AXL signaling in metastatic tumor cells is sufficient to suppress tumor cell migration in vitro (12–17). In vivo, a role for AXL in invasion and metastasis has recently been described in breast and glioma tumor models (15, 17–19). MMP-9 has recently been identified as an important effector of AXL-mediated invasion. MMP-9 expression is affected by both overexpression and down regulation of AXL in breast and pancreatic tumor cells (14, 16). These studies demonstrate that AXL is an important factor for tumor cell invasion and metastasis, however the role of AXL in ovarian cancer growth and progression remains unknown and importantly the efficacy of a therapeutic agent specifically targeting AXL in metastatic disease remains largely untested.

In this study, we test the hypothesis that AXL is a critical factor for ovarian tumor metastasis and that therapeutic blockade of AXL signaling may be an effective treatment for metastatic ovarian cancer. We utilize both genetic and therapeutic approaches to directly assess the role of AXL in the initiation and progression of metastatic ovarian cancer. This study demonstrates that AXL is a therapeutic target for human ovarian cancer and shows that a

specific therapeutic agent targeting AXL is sufficient to significantly inhibit metastatic tumor progression without normal tissue toxicity.

Materials and Methods

Cell Lines

Ovarian SKOV3, SKOV3ip.1, and HEYA8 cells were obtained as a gift from Dr. Gordon Mills (MD Anderson Cancer Center). Ovarian ES-2 and MESOV cells were a gift from Dr. Branimir Sikic (Stanford University). OVCAR-3 cells were purchased from ATCC. IGROV-1 and OVCAR-8 cells were purchased from the NCI-Frederick DCTD tumor cell line repository. All cell lines were authenticated from the original source and were used within 6 months of receipt. Additionally, cells were tested upon receipt for viability, cell morphology, and the presence of mycoplasma and viruses including MPV, MVM, MHV, Ectromelia, MAV-1, -2; Reo 1&3, LCMV, LDH, and TMEV (Charles River Laboratories). Cells were cultured in the appropriate media supplemented with 10% heat inactivated fetal bovine serum and 1% penicillin and streptomycin at 37°C in a 5% CO_2 incubator.

shRNA Constructs

Oligos for AXL shRNA were synthesized as previously described (20) 5'-GATTTGGAGAACACACTGA-3'. A scramble sequence was used as a non-targeting shRNA 5'-AATTGTACTACACAAAAGTAC-3'. Oligos were cloned into the pSiren RetroQ (BD Bioscience) vector. Infected cells were selected in puromycin (Sigma) and polyclonal populations were tested for decreased AXL expression levels by western blot analysis.

Plasmids

The AXL ectodomain (amino acids 1–451) was amplified from the human AXL cDNA (Open Biosystems) and cloned into the CMV-driven pADD2 adenoviral shuttle vector. Transient transfections with control vector or AXL ectodomain were performed with Lipofectamine 2000 (Invitrogen) into HCT116 cells. Conditioned media was collected 48–72 hours following transfection.

Generation and Production of Adenovirus

The AXL ectodomain (aa 1–451) was cloned into the E1 region of E1⁻E3⁻ Ad strain 5 by homologous recombination followed by adenovirus production in 293 cells and CsCl gradient purification as previously described (21). The production and purification of the sAXL adenovirus and the negative control virus expressing murine $IgG2_\alpha$-Fc immunoglobulin fragment was performed as previously described (21).

Growth of SKOV3ip.1 and OVCAR-8 Cells as Peritoneal and Subcutaneous Xenografts

All procedures involving animals and their care were approved by the Institutional Animal Care and Usage Committee of Stanford University in accordance with institutional and NIH guidelines.

For genetic studies, shSCRM and shAXL SKOV3ip.1 and OVCAR-8 cells were injected i.p. with 1×0^6 and 5×10^6 cells respectively in 0.5 ml of PBS into female nude mice. After sacrifice, the presence of ascites was identified, metastatic lesions were counted and all visible lesions were dissected and removed to determine total tumor weight.

For therapeutic studies, SKOV3ip.1 and OVCAR-8 parental cells were injected i.p. with 1×10^6 and 5×10^6 cells respectively in 0.5 ml of PBS into female nude mice. Seven

(SKOV3ip.1) or 14 (OVCAR-8) days following tumor cell injection, mice were injected with sAXL or control 1.9×10^8 adenoviral pfu in 0.1ml PBS into the tail vein.

For subcutaneous tumors, 5 million cells in 0.1 ml of PBS were implanted subcutaneously into the flanks nude (*nu/nu*) six-week-old female mice. Tumors were measured with calipers over a 45-day time course. Volume was calculated using the following formula: width$^2 \times$ length $\times$ 0.5.

Tissue Toxicity Studies

Blood was collected from tumor bearing Ad-Fc or Ad-sAXL treated mice. Comprehensive metabolic panel and CBC analysis was performed by the Department of Comparative Medicine at Stanford University. Tissue samples were collected from all major organs including liver, kidney, brain, and spleen, fixed in 10% formalin, embedded in paraffin, sectioned and counter stained with hematoxylin and eosin.

Statistical Analysis

Statistical analysis of AXL expression in human tissue samples was performed using the Fisher's Exact test. All other statistical tests were performed using the Student's t test. Values with a p value of < 0.05 were considered statistically significant.

Results

AXL is a marker of Type II ovarian cancer and metastasis

We first compared AXL expression in normal ovarian tissue, primary tumor, and metastases. AXL expression was first examined in specimens of normal ovarian surface epithelium (OSE) taken from patients with benign ovarian disease since the majority of ovarian tumors are thought to arise from OSE (22). AXL was expressed in 0% (0/10) of specimens with normal OSE (Table I and Figure 1). In contrast, 73% (219/297) of all ovarian tumor samples including both Type I and Type II tumors were positive for membranous AXL staining in the epithelium demonstrating that AXL expression is significantly higher (P<0.0001) in ovarian carcinomas than normal ovarian epithelium (Figure 1 and Table I). Additionally, we found that the number of cases with positive AXL staining (score of 2 or 3) was significantly higher in Type II (high-grade serous and high-grade endometrioid) than Type I (low-grade serous and low-grade endometrioid) primary tumors (p < 0.0001, Table I). Type I tumors usually present at low stage and are not aggressive whereas Type II tumors present at advanced stage and are highly aggressive indicating that AXL expression correlates with aggressive behavior in Type II ovarian tumors (23). Furthermore, metastatic tumor samples collected from the omentum and peritoneum of serous ovarian cancer patients showed high AXL expression in 75% (24/32) and 90% (27/30) of specimens respectively (Figure 1 and Table I). These findings demonstrate that AXL expression is significantly induced in aggressive ovarian tumors and its expression is maintained at high levels in ovarian tumor metastases.

AXL is a critical factor for ovarian tumor metastasis

To examine the functional role of AXL in metastasis, we utilized a genetic approach to inhibit AXL in mouse models of ovarian metastasis. For this purpose, we screened a panel of human ovarian cancer cell lines for AXL protein expression in order to identify metastatic cell lines with high levels of AXL expression. Similar to our clinical findings, AXL was highly expressed in the majority of metastatic ovarian (SKOV3, OVCAR-8, ES-2, MESOV, HEYA8) cell lines, whereas AXL was expressed at undetectable or low levels in cell lines with low metastatic potential (IGROV1 and OVCAR-3, Figure 2A). AXL deficient metastatic ovarian (SKOV3ip.1 and OVCAR-8) cell lines were generated using previously

described AXL shRNA targeting sequences (20). Western blot analysis confirmed that cells expressing shAXL targeting sequences expressed less than 5% of AXL protein compared to cells expressing the scramble control shRNA targeting sequence (shSCRM, Figure 2B).

We first examined if AXL plays a general role in the regulation of ovarian tumor cell proliferation and growth. To address these questions, we performed in vitro proliferation assays in which total cell numbers between AXL wild type (shSCRM) and AXL deficient (shAXL) cells were counted over a 10–14 day period. We found no significant difference in cellular growth curves between shSCRM and shAXL SKOV3ip.1 or OVCAR-8 cells in vitro (Figure 2C). Similarly, no significant difference was observed in subcutaneous growth of shSCRM and shAXL SKOV3ip.1 cells (Figure 2D). These findings indicate that AXL is not required for ovarian tumor cell proliferation or subcutaneous growth.

To determine whether genetic inactivation of AXL affects the ability of ovarian cancer cells to metastasize in vivo, we compared the ability of shSCRM and shAXL SKOV3ip.1 and OVCAR-8 cells to form metastases using the peritoneal xenograft model of ovarian cancer. This model recapitulates the peritoneal dissemination of human ovarian metastases in which nude mice develop rapidly progressive disease consisting of ascites and more than 100 small metastatic lesions attached to the mesentery, diaphragm, liver, and other peritoneal surfaces following peritoneal injection of metastatic human ovarian tumor cells (24). Immunohistochemical analysis of AXL expression in SKOV3ip.1 peritoneal metastases revealed that similar to human ovarian metastases, AXL is highly expressed in SKOV3ip.1 metastatic lesions, confirming that this is a relevant model system to investigate the role of AXL in ovarian metastasis (Figure 3A). Twenty-eight days following peritoneal injection of shSCRM or shAXL cells, shSCRM mice displayed signs of severe ascites and morbidity necessitating us to sacrifice the mice and investigate changes in tumor burden between the shSCRM and shAXL injected mice. While mice injected with shSCRM cells developed ascites and >100 peritoneal metastases, mice injected with shAXL cells developed very few metastases (Figure 3B). The average number of peritoneal metastases greater than 5mm in size was significantly reduced from 13.4+/− 4.3 in shSCRM injected mice to 0.8+/− 0.5 in shAXL injected mice (Figure 3B). Similarly, the average weight of these tumors was significantly reduced from 236 +/− 74 mg in shSCRM-injected mice to 39.2 +/−18 mg in shAXL-injected mice (Figure 3B). In support of these findings, knockdown of AXL expression in OVCAR-8 cells significantly inhibited total ovarian peritoneal tumor mass and tumor number in mice injected with these cells (Figure 3C). Collectively, these findings demonstrate that AXL is a critical factor for the establishment of ovarian tumor metastasis.

AXL regulates ovarian tumor cell invasion

To determine a mechanism for AXL-mediated metastasis, we took an unbiased approach and directly compared the role of AXL in the critical cellular functions associated with the metastatic cascade including proliferation, invasion, migration, adhesion, and survival (5). We found that shAXL SKOV3ip.1 and OVCAR-8 cells were significantly impaired in the ability to invade through type I collagen (Figure 4). We also observed a modest decrease in cellular migration in shAXL cells, yet we were unable to find a difference in adhesion to ECM proteins or survival following serum withdrawal indicating that AXL predominately affects invasion in the metastatic cascade (Supplementary Figure 1).

Matrix metalloproteinases MMP-1, -2, and -9 are key contributors to ovarian tumor cell invasion and progression (25). Therefore, we investigated whether AXL regulates the expression and/or activity of these enzymes in human ovarian cancer cells. Using shSCRM and shAXL OVCAR-8 and SKOV3ip.1 cells, we found that AXL regulates the expression of all three MMPs in human ovarian cancer cells. Loss of AXL significantly reduced the expression of MMP-1 and MMP-2 in SKOV3ip.1 cells (Figure5A). Similarly, in OVCAR-8

cells MMP-1 and MMP-9 expression was significantly reduced in AXL deficient cells (Figure 5A). A recent report demonstrated a role for MMP-9 in AXL mediated invasion in breast cancer cells (14). Therefore, we focused on the role of AXL in the regulation of MMP-2 in ovarian cancer. Luciferase reporter assays revealed that MMP-2 promoter activity was significantly decreased in shAXL cells compared to shSCRM cells indicating that AXL regulates MMP-2 at the transcriptional level (Figure 5B). Gelatin zymography assays indicated that MMP-2 secreted protein levels were also significantly reduced in shAXL cells compared to shSCRM SKOV3ip.1 cells (Figure 5C). Collectively, these findings suggest a role for AXL as an upstream regulator of MMP expression and activity in human ovarian cancer cells.

We next sought to elucidate the signaling pathways involved in AXL-mediated MMP expression. Activation of AXL by GAS6 has been reported to directly induce a number of intracellular signaling pathways including PI3K, RAS, MAPK, SRC, and PLC (for recent review, (11)). Among these pathways, the PI3K/AKT signaling pathway has been shown to regulate MMP-2 expression and invasion in ovarian cancer cells (26, 27). To determine whether PI3K signaling is affected by loss of AXL in SKOV3ip.1 cells, we performed western blot analysis for phospho-AKT at Ser473 (P-AKT) in AXL-wild type and AXL-deficient SKOV3ip.1 cells. We found a profound inhibition of P-AKT expression in shAXL cells compared to shSCRM SKOV3ip.1 cells (Figure 5D). Additionally, GAS6 stimulation of starved SKOV3ip.1 cells resulted in a PI3K-dependent induction of P-AKT as treatment with the PI3K inhibitor Ly294002 completely abrogated GAS6-induced P-AKT expression (Figure 5D). The MAPK/ERK pathway has also been shown to regulate MMP expression, however inactivation of AXL in shAXL SKOV3ip.1 cells did not affect phospho-ERK1/2 levels indicating that AXL may regulate MMP-2 expression through the PI3K/AKT signaling pathway (Supplementary Figure 2).

Therapeutic inhibition of AXL significantly suppresses metastatic tumor progression in mice

Our findings thus far demonstrate that AXL is a critical factor for ovarian metastasis and support the hypothesis that therapeutic blockade may be an effective treatment for metastatic disease. To test this hypothesis, we utilized the soluble human AXL ectodomain as a therapeutic strategy to inhibit AXL signaling. The soluble AXL ectodomain functionally acts as a decoy receptor and has previously been shown to bind GAS6 with nanomolar affinity (28, 29) (Supplementary Figure 3). We first examined whether treatment with soluble AXL ectodomains is sufficient to inhibit AXL signaling and invasion in metastatic tumor cells. We and others have shown that the PI3K/AKT signaling is regulated by AXL in a variety of cell types (Figure5D, (11)). Treatment with soluble AXL ectodomains (sAXL) was able to reduce PI3K/AKT activation in GAS6 treated SKOV3ip.1 cells (Supplementary Figure 3B). Additionally, treatment of metastatic tumors cells in collagen with sAXL was sufficient to dramatically reduce cellular invasion demonstrating that sAXL treatment inhibits AXL signaling and invasion in vitro (Supplementary Figure 3C).

We next examined whether sAXL treatment would affect metastatic tumor progression in highly metastatic models of ovarian cancer. We first established SKOV3ip.1 metastatic lesions in nude mice (day 1) and began treatment with sAXL at day 7 following verification of macroscopic lesions. sAXL therapy was delivered using an adenoviral system in which the liver releases systemic production of sAXL protein into the serum of mice for up to 28 days following injection (Figure 6A, (30)). Macroscopic analysis of tumor burden at day 28 revealed that mice receiving sAXL therapy had a significant (p < 0.01) reduction in tumor burden compared to mice treated with the Fc control therapy. In the SKOV3ip.1 tumor model, total tumor weight and tumor number was decreased by 63% in mice treated with sAXL compared to Fc treated mice (Figure 6B). Similarly in the OVCAR-8 tumor model,

total tumor weight and tumor number was significantly decreased by 47% and 42% with sAXL therapy respectively (Supplementary Figure 4). We examined MMP-2 expression levels in SKOV3ip.1 tumors by real time PCR analysis and found that MMP-2 levels were significantly decreased in the tumors of sAXL treated mice compared to Fc control treated mice (Figure 6C). Given that previous anti-metastatic inhibitors that target MMPs have been shown to have significant effects on normal tissue toxicity, we performed a comprehensive analysis of normal tissue toxicity in mice treated with sAXL therapy for 21 days. We observed no behavioral, macroscopic, or microscopic abnormalities in nude mice treated with sAXL or Fc therapy (Supplementary Figures 5 and 6, data not shown). These results demonstrate that a single agent AXL therapy is sufficient to significantly reduce metastatic tumor burden in mice with established disease without normal tissue toxicity. In addition, our findings suggest that the therapeutic effect of AXL on metastatic tumor growth may involve the inhibition of invasion at least in part through the regulation of MMP activity.

Discussion

In this report, we demonstrate that advanced Type II and metastatic ovarian tumor cells dramatically increase AXL receptor surface expression and are critically dependent on the GAS6/AXL signaling cascade for successful metastatic colonization. Our findings indicate that the PI3K/AKT signaling pathway may be an important component of the GAS6/AXL signaling cascade regulating ovarian tumor metastasis. Although genetic mutations in the PTEN/PI3K pathway are rare in Type II ovarian tumors (23), phosphorylation and activation of AKT1 and AKT2 is a common event in high-grade and advanced stage ovarian tumors (31, 32). Proposed mechanisms for AKT activation in these tumors include increased protein expression, activated RAS, as well as activated receptor signaling pathways (31, 33). Our study identifies GAS6/AXL signaling as a novel mechanism for AKT activation in advanced ovarian tumors. PI3K/AKT controls metastasis by increasing the expression of proteolytic enzymes including MMP-2 and MMP-9 resulting in the destruction of the extracellular matrix and enhanced tumor cell invasion (26, 27). Given the important role of PI3K/AKT and MMP pathways in ovarian tumor progression and metastasis, the development of therapeutic agents targeting these pathways is important for the treatment of cancer. PI3K inhibitors wortmannin and LY294002 have been developed and are commonly used to inhibit tumor cell proliferation and tumor growth. However, given the poor solubility and the high toxicity due to the broad range of PI3K-related enzymes targeted by these compounds, these agents have had very limited clinical applications to date (34). AKT and MMP inhibitors have been tested in clinical trials for a variety of human cancers, however the clinical outcomes from these studies were not satisfied and tissue toxicities were observed (for recent reviews (35)). Here we show that therapeutic blockade of GAS6/AXL signaling using soluble receptors is a highly specific and non-toxic strategy to inhibit PI3K/AKT, MMP-2, invasion, and metastasis in metastatic ovarian tumor cells.

AXL is a non-essential therapeutic target

Analysis of AXL expression in normal tissues demonstrates that AXL is expressed in neural, lymphoid, myeloid, vascular, and reproductive tissues (36–41). However, analysis of Axl and Gas6 germline knockout mice demonstrates that the GAS6/AXL signaling cascade is not required for embryonic development or normal tissue function (41, 42). Under pathophysiologic conditions of acute anemia, Gas6 and Axl deficient mice have impaired erythropoiesis indicating a role for GAS/AXL signaling in the generation of erythroid progenitors and erythroblasts under these conditions (43). While these studies demonstrate that genetic inactivation of GAS6/AXL signaling has minimal effects on normal tissue function, the effects of anti-AXL therapy on normal tissue function has not been tested in pre-clinical models of metastasis. Our study demonstrates that therapeutic blockade of

GAS6/AXL signaling using soluble AXL receptors does not induce tissue or hematological toxicity in mice.

Single agent anti-AXL therapy is sufficient to suppress metastatic ovarian tumor progression

We show that single-agent AXL therapy is sufficient to inhibit metastatic tumor progression in highly metastatic models of metastatic ovarian cancer. These findings have important clinical implications for the treatment of ovarian cancer. Currently there are no FDA approved targeted-therapies for the treatment of ovarian cancer, although several classes of inhibitors targeting EGFR, VEGF, PDGFR, and Src are in clinical trials for the treatment of advanced and recurrent ovarian cancer ((44), clinical trials.gov). Standard therapy for ovarian cancer includes surgery with optimal debulking of disease followed by cytotoxic platinum-taxane combination therapy. Despite these efforts, eighty percent of patients diagnosed with ovarian cancer develop recurrent disease and only 30% of these patients survive 5 years following diagnosis. Our data suggest that AXL therapy may be an effective adjuvant therapy for the treatment of advanced and recurrent ovarian cancer. The model of metastatic ovarian tumor progression used in our studies resembles the development of recurrent disease in human patients following surgical debulking. We found that AXL therapy was able to reduce metastatic tumor burden in mice with established disease by 63%. While the growth of established tumors was only modestly affected by AXL therapy, the establishment of new metastatic lesions during the progression of disease was significantly reduced. Taken together our results indicate that AXL therapy appears to function primarily as an anti-metastatic agent and may be most effective as a combination therapy with current cytotoxic agents. Interestingly, AXL has also been linked to resistance to chemotherapeutic drugs suggesting that anti-AXL therapy in combination with cytotoxic drugs may not only inhibit metastatic spread, but may also enhance the efficacy of chemotherapy (45, 46).

In summary, AXL is an important therapeutic target for metastatic ovarian cancer. This study demonstrates using soluble human AXL receptors that an AXL-specific therapy is sufficient to significantly reduce metastatic tumor progression in vivo using aggressive models of ovarian cancer. These findings have direct clinical implications for the treatment of ovarian cancer for which current therapies are ineffective and demonstrate that an AXL specific inhibitor is an effective and non-toxic strategy for the treatment of metastatic disease.

Supplementary Material

Refer to Web version on PubMed Central for supplementary material.

Acknowledgments

References

1. Naora H, Montell DJ. Ovarian cancer metastasis: integrating insights from disparate model organisms. Nat Rev Cancer. 2005; 5:355–66. [PubMed: 15864277]

2. Tan DS, Agarwal R, Kaye SB. Mechanisms of transcoelomic metastasis in ovarian cancer. Lancet Oncol. 2006; 7:925–34. [PubMed: 17081918]

3. Shan W, Liu J. Inflammation: a hidden path to breaking the spell of ovarian cancer. Cell Cycle. 2009; 8:3107–11. [PubMed: 19738436]

4. Kim MY, Oskarsson T, Acharyya S, et al. Tumor self-seeding by circulating cancer cells. Cell. 2009; 139:1315–26. [PubMed: 20064377]

5. Sahai E. Illuminating the metastatic process. Nat Rev Cancer. 2007; 7:737–49. [PubMed: 17891189]

6. Bonome T, Lee JY, Park DC, et al. Expression profiling of serous low malignant potential, low-grade, and high-grade tumors of the ovary. Cancer Res. 2005; 65:10602–12. [PubMed: 16288054]

7. Lancaster JM, Dressman HK, Clarke JP, et al. Identification of genes associated with ovarian cancer metastasis using microarray expression analysis. Int J Gynecol Cancer. 2006; 16:1733–45. [PubMed: 17009964]

8. Liu AX, Testa JR, Hamilton TC, Jove R, Nicosia SV, Cheng JQ. AKT2, a member of the protein kinase B family, is activated by growth factors, v-Ha-ras, and vsrc through phosphatidylinositol 3-kinase in human ovarian epithelial cancer cells. Cancer Res. 1998; 58:2973–7. [PubMed: 9679957]

9. O'Bryan JP, Frye RA, Cogswell PC, et al. axl, a transforming gene isolated from primary human myeloid leukemia cells, encodes a novel receptor tyrosine kinase. Mol Cell Biol. 1991; 11:5016–31. [PubMed: 1656220]

10. Nagata K, Ohashi K, Nakano T, et al. Identification of the product of growth arrest-specific gene 6 as a common ligand for Axl, Sky, and Mer receptor tyrosine kinases. J Biol Chem. 1996; 271:30022–7. [PubMed: 8939948]

11. Linger RM, Keating AK, Earp HS, Graham DK. TAM receptor tyrosine kinases: biologic functions, signaling, and potential therapeutic targeting in human cancer. Adv Cancer Res. 2008; 100:35–83. [PubMed: 18620092]

12. Zhang YX, Knyazev PG, Cheburkin YV, et al. AXL is a potential target for therapeutic intervention in breast cancer progression. Cancer Res. 2008; 68:1905–15. [PubMed: 18339872]

13. Shieh YS, Lai CY, Kao YR, et al. Expression of axl in lung adenocarcinoma and correlation with tumor progression. Neoplasia. 2005; 7:1058–64. [PubMed: 16354588]

14. Tai KY, Shieh YS, Lee CS, Shiah SG, Wu CW. Axl promotes cell invasion by inducing MMP-9 activity through activation of NF-kappaB and Brg-1. Oncogene. 2008; 27:4044–55. [PubMed: 18345028]

15. Vajkoczy P, Knyazev P, Kunkel A, et al. Dominant-negative inhibition of the Axl receptor tyrosine kinase suppresses brain tumor cell growth and invasion and prolongs survival. Proc Natl Acad Sci U S A. 2006; 103:5799–804. [PubMed: 16585512]

16. Koorstra JB, Karikari CA, Feldmann G, et al. The Axl receptor tyrosine kinase confers an adverse prognostic influence in pancreatic cancer and represents a new therapeutic target. Cancer Biol Ther. 2009; 8:618–26. [PubMed: 19252414]

17. Li Y, Ye X, Tan C, et al. Axl as a potential therapeutic target in cancer: role of Axl in tumor growth, metastasis and angiogenesis. Oncogene. 2009

18. Gjerdrum C, Tiron C, Hoiby T, et al. Axl is an essential epithelial-tomesenchymal transition-induced regulator of breast cancer metastasis and patient survival. Proc Natl Acad Sci U S A. 107:1124–9. [PubMed: 20080645]

19. Holland SJ, Pan A, Franci C, et al. R428, a selective small molecule inhibitor of axl kinase, blocks tumor spread and prolongs survival in models of metastatic breast cancer. Cancer Res. 70:1544–54. [PubMed: 20145120]

20. Holland SJ, Powell MJ, Franci C, et al. Multiple roles for the receptor tyrosine kinase axl in tumor formation. Cancer Res. 2005; 65:9294–303. [PubMed: 16230391]

21. Kuo CJ, Farnebo F, Yu EY, et al. Comparative evaluation of the antitumor activity of antiangiogenic proteins delivered by gene transfer. Proc Natl Acad Sci U S A. 2001; 98:4605–10. [PubMed: 11274374]

22. Feeley KM, Wells M. Precursor lesions of ovarian epithelial malignancy. Histopathology. 2001; 38:87–95. [PubMed: 11207821]

23. Kurman RJ, Shih Ie M. The origin and pathogenesis of epithelial ovarian cancer: a proposed unifying theory. Am J Surg Pathol. 2010; 34:433–43. [PubMed: 20154587]

24. Yoneda J, Kuniyasu H, Crispens MA, Price JE, Bucana CD, Fidler IJ. Expression of angiogenesis-related genes and progression of human ovarian carcinomas in nude mice. J Natl Cancer Inst. 1998; 90:447–54. [PubMed: 9521169]

25. Egeblad M, Werb Z. New functions for the matrix metalloproteinases in cancer progression. Nat Rev Cancer. 2002; 2:161–74. [PubMed: 11990853]

26. Nielsen-Preiss SM, Allen MP, Xu M, et al. Adhesion-related kinase induction of migration requires phosphatidylinositol-3-kinase and ras stimulation of rac activity in immortalized gonadotropin-releasing hormone neuronal cells. Endocrinology. 2007; 148:2806–14. [PubMed: 17332061]

27. Choi JH, Choi KC, Auersperg N, Leung PC. Gonadotropins activate proteolysis and increase invasion through protein kinase A and phosphatidylinositol 3-kinase pathways in human epithelial ovarian cancer cells. Cancer Res. 2006; 66:3912–20. [PubMed: 16585220]

28. Sasaki T, Knyazev PG, Cheburkin Y, et al. Crystal structure of a C-terminal fragment of growth arrest-specific protein Gas6. Receptor tyrosine kinase activation by laminin G-like domains. J Biol Chem. 2002; 277:44164–70. [PubMed: 12218057]

29. Budagian V, Bulanova E, Orinska Z, et al. Soluble Axl is generated by ADAM10-dependent cleavage and associates with Gas6 in mouse serum. Mol Cell Biol. 2005; 25:9324–39. [PubMed: 16227584]

30. Kuhnert F, Tam BY, Sennino B, et al. Soluble receptor-mediated selective inhibition of VEGFR and PDGFRbeta signaling during physiologic and tumor angiogenesis. Proc Natl Acad Sci U S A. 2008; 105:10185–90. [PubMed: 18632559]

31. Mills GB, Lu Y, Fang X, et al. The role of genetic abnormalities of PTEN and the phosphatidylinositol 3-kinase pathway in breast and ovarian tumorigenesis, prognosis, and therapy. Semin Oncol. 2001; 28:125–41. [PubMed: 11706404]

32. Yuan ZQ, Sun M, Feldman RI, et al. Frequent activation of AKT2 and induction of apoptosis by inhibition of phosphoinositide-3-OH kinase/Akt pathway in human ovarian cancer. Oncogene. 2000; 19:2324–30. [PubMed: 10822383]

33. Guo RX, Qiao YH, Zhou Y, Li LX, Shi HR, Chen KS. Increased staining for phosphorylated AKT and nuclear factor-kappaB p65 and their relationship with prognosis in epithelial ovarian cancer. Pathol Int. 2008; 58:749–56. [PubMed: 19067848]

34. Marone R, Cmiljanovic V, Giese B, Wymann MP. Targeting phosphoinositide 3-kinase: moving towards therapy. Biochim Biophys Acta. 2008; 1784:159–85. [PubMed: 17997386]

35. Coussens LM, Fingleton B, Matrisian LM. Matrix metalloproteinase inhibitors and cancer: trials and tribulations. Science. 2002; 295:2387–92. [PubMed: 11923519]

36. Fridell YW, Villa J Jr. Attar EC, Liu ET. GAS6 induces Axl-mediated chemotaxis of vascular smooth muscle cells. J Biol Chem. 1998; 273:7123–6. [PubMed: 9507025]

37. Caraux A, Lu Q, Fernandez N, et al. Natural killer cell differentiation driven by Tyro3 receptor tyrosine kinases. Nat Immunol. 2006; 7:747–54. [PubMed: 16751775]

38. Prieto AL, Weber JL, Lai C. Expression of the receptor protein-tyrosine kinases Tyro-3, Axl, and mer in the developing rat central nervous system. J Comp Neurol. 2000; 425:295–314. [PubMed: 10954847]

39. Sharif MN, Sosic D, Rothlin CV, et al. Twist mediates suppression of inflammation by type I IFNs and Axl. J Exp Med. 2006; 203:1891–901. [PubMed: 16831897]

40. Lu Q, Lemke G. Homeostatic regulation of the immune system by receptor tyrosine kinases of the Tyro 3 family. Science. 2001; 293:306–11. [PubMed: 11452127]

41. Lu Q, Gore M, Zhang Q, et al. Tyro-3 family receptors are essential regulators of mammalian spermatogenesis. Nature. 1999; 398:723–8. [PubMed: 10227296]

42. Angelillo-Scherrer A, de Frutos P, Aparicio C, et al. Deficiency or inhibition of Gas6 causes platelet dysfunction and protects mice against thrombosis. Nat Med. 2001; 7:215–21. [PubMed: 11175853]

43. Angelillo-Scherrer A, Burnier L, Lambrechts D, et al. Role of Gas6 in erythropoiesis and anemia in mice. J Clin Invest. 2008; 118:583–96. [PubMed: 18188450]

44. Dupont J, Aghajanian C, Sabbatini P, Spriggs DR. New agents for the treatment of ovarian cancer: the next generation. Int J Gynecol Cancer. 2005; 15(Suppl 3):252–7. [PubMed: 16343241]

45. Lay JD, Hong CC, Huang JS, et al. Sulfasalazine suppresses drug resistance and invasiveness of lung adenocarcinoma cells expressing AXL. Cancer Res. 2007; 67:3878–87. [PubMed: 17440102]

46. Hong CC, Lay JD, Huang JS, et al. Receptor tyrosine kinase AXL is induced by chemotherapy drugs and overexpression of AXL confers drug resistance in acute myeloid leukemia. Cancer Lett. 2008; 268:314–24. [PubMed: 18502572]
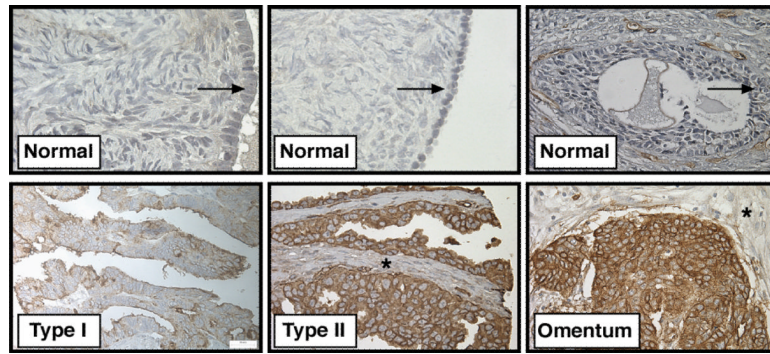
Figure 1. AXL is highly expressed in Type II ovarian tumors and metastases
Representative images of AXL immunohistochemical staining in normal ovarian epithelium (arrow), Type I (low-grade) serous, Type II (high-grade) serous, and omental metastases derived from patients with serous adenocarcinoma. Note that normal and tumor stroma were negative for AXL staining (*). Scale bar represents 20 ums.
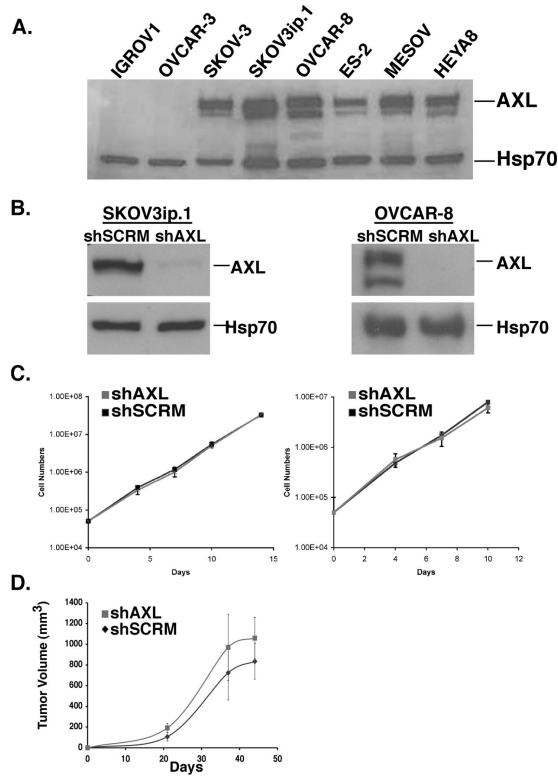
Figure 2. Genetic inactivation of AXL does not affect ovarian tumor cell proliferation in vitro or subcutaneous growth in vivo
A. Western blot analysis of AXL expression in a panel of human ovarian cancer cell lines.
B. Western blot analysis of AXL expression in SKOV3ip.1 and OVCAR-8 cells stably transfected with shRNA targeting sequences for scramble control (shSCRM) or AXL (shAXL). Heat shock protein 70 (Hsp70) was used as a protein loading control. **C.** Cellular growth curves for SKOV3ip.1 (left), and OVCAR-8 (right) shSCRM) and shAXL cells (n = 3). Error bars represent the S.E.M. **D.** Average tumor volumes of subcutaneous SKOV3ip.1 tumors (n = 4 mice per group) grown over a 48-day time course. Error bars represent the S.E.M.. All full-length blots are presented this figure are in Supplementary Figure 7.
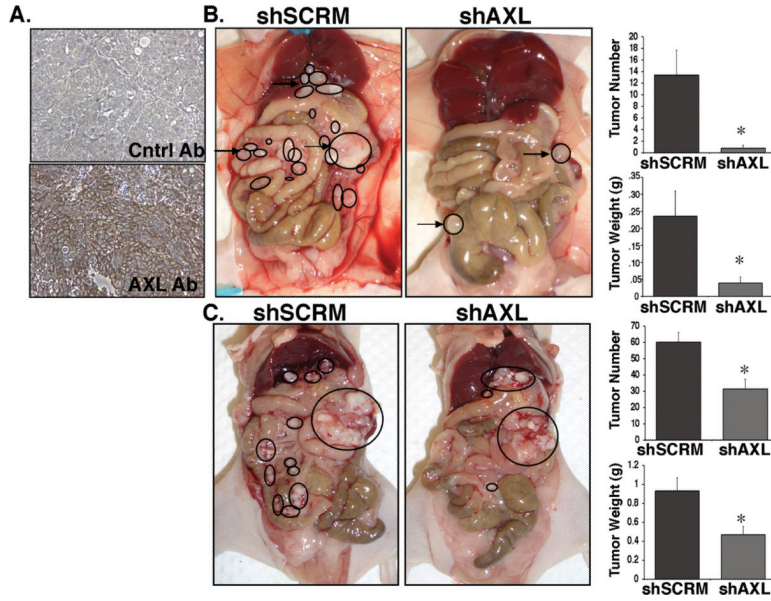
Figure 3. Genetic inactivation of AXL is sufficient to inhibit the initiation of ovarian metastasis
A. AXL immunohistochemical staining (bottom) in peritoneal metastatic lesions from mice injected with shSCRM SKOV3ip.1 cells. **B.** Representative photographs of mice taken 28 days after injection with shSCRM) and shAXL SKOV3ip.1 cells. Note that the shSCRM injected mice developed numerous metastases in throughout the abdominal cavity (circled). For the shAXL group, the mouse with the greatest tumor burden is shown. Graphs depict the average number of peritoneal metastases >5mm in size per mouse and the average weight of the largest tumor (n = 5 per group). **C.** Photographs of mice taken 34 days after injection with shSCRM and shAXL OVCAR-8 cells. Note that the shSCRM injected mice developed numerous metastases throughout the abdominal cavity (circled). Large circles represent the original tumor explant inoculation. Graphs depict the average number of peritoneal metastases per mouse and the average tumor weight (n = 8). Asterisks indicate a significant change in tumor burden as determined by the student's t-test (*, $p < 0.05$).
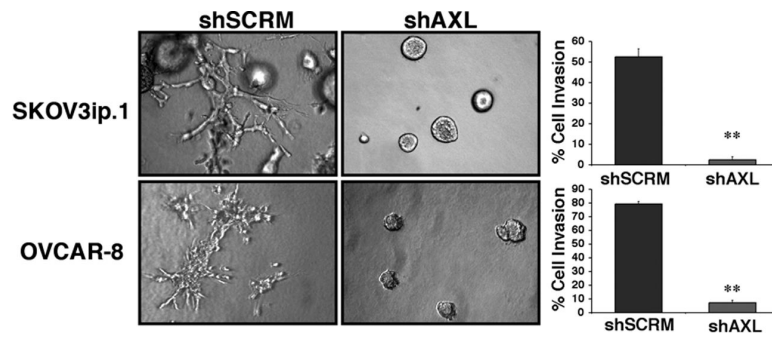
Figure 4. AXL regulates ovarian tumor cell invasion
Collagen invasion assays of shSCRM and shAXL SKOV3ip.1 and OVCAR-8 cells.
Photographs were taken 7 days after plating cells in collagen. Note the invasive phenotype
observed in AXL wild type cells (branching) compared to AXL deficient cells (rounded).
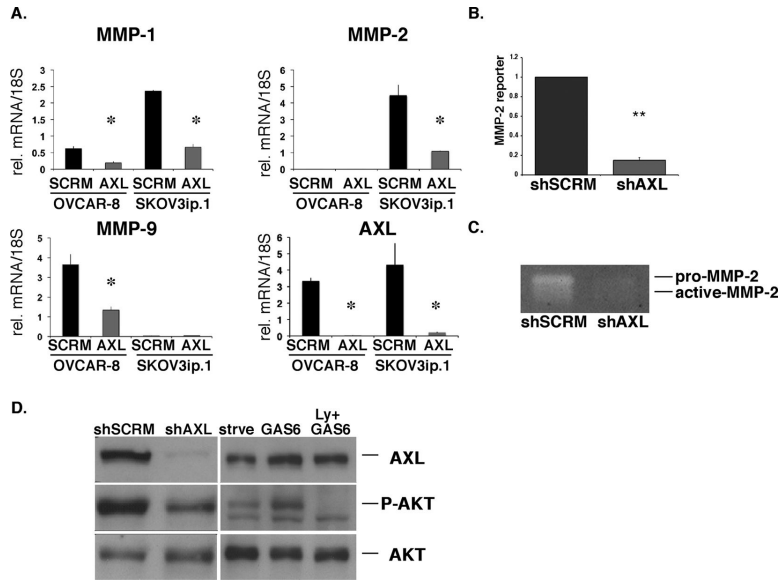Graphs show quantification of collagen invasion assays (n = 9).

Figure 5. AXL regulates the PI3K/AKT signaling pathway and MMP expression in ovarian cancer cells

A. Real time PCR analysis of MMP-1, -2, -9, and AXL expression in shAXL and shSCRM ovarian tumor cells. Expression values were normalized to 18S; n = 3. Error bars represent the S.E.M.. **B.** MMP-2 reporter assay of shSCRM or shAXL SKOV3ip.1 cells (n = 6). **C.** Gelatin zymography assay for pro- and active-MMP2 activity in conditioned media collected from serum starved SKOV3ip.1 cells. **D.** Western blot analysis of phospho-AKT at Ser473 (P-AKT), total AKT (AKT), and AXL expression in SKOV3ip.1 cells expressing shRNA sequences targeting shSCRM or shAXL and starved SKOV3ip.1 cells (strve) treated with GAS6 alone or the PI3K inhibitor Ly294002 (Ly). Asterisks indicate a significant increase or decrease in invasion or expression compared to shSCRM as determined by the student's t-test (*, p < 0.01; **, p < 0.001). All full-length blots are presented this figure are in Supplementary Figure 8.
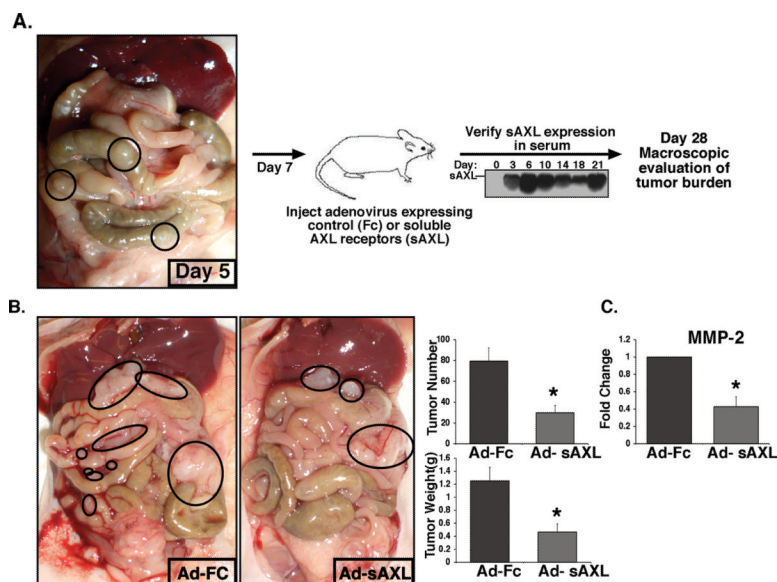
Figure 6. Treatment with soluble AXL receptors inhibits metastatic tumor burden in mice with established metastases

A. Schematic representation of the soluble AXL receptor treatment study. Nude mice were i.p. injected with 1X10e6 SKOV3ip.1 cells. Five days later, the presence of macroscopic lesions was verified in mice. At day 7, mice were injected with adenoviruses expressing the IgG2α-Fc control (Ad-Fc) or soluble AXL receptor (Ad-sAXL). sAXL serum levels were assessed by western blot every 3–4 days following adenoviral injection. Day 28 following tumor cell implantation tumor burden was assessed in all mice. **B.** Representative photographs of mice treated with AdsAXL or Ad-Fc at day 28. Metastatic lesions are circled. Graphs show the average total tumor number and weight (n = 7). Error bars represent the S.E.M. A statistical difference in tumor number and weight (p=0.01) was observed between Ad-Fc and Ad-sAXL treated mice (*). **C.** Real time PCR analysis of MMP-2 expression in tumors of mice treated with Ad-Fc or Ad-AXL. All full-length blots are presented in Supplementary Figure 9.

Table 1

AXL expression in human ovarian cancer

Immunohistochemical analysis of AXL staining in normal ovary, human ovarian primary tumors, and metastases.

Analysis of AXL Staining to Ovarian Tumor Parameters

Score	0	1	2	3	Total
Normal Ovary	10 (100)	0 (0)	0 (0)	0 (0)	10
Mucinous	14 (61)	3 (13)	4 (17)	2 (9)	23
Clear Cell	11 (44)	0 (0)	12 (48)	2 (8)	25
Type I					
Low Grade Serous	31 (42)	1 (1)	33 (45)	9 (12)	74
Low Grade Endometrioid	1 (11)	2 (22)	5 (55)	1 (11)	9
Totals	32	3	38	10	83
Type II					
High Grade Serous	14 (9)	6 (4)	44 (28)	95 (60)	159
High Grade Endometrioid	7 (30)	4 (17)	7 (30)	5 (15)	23
Totals	21	10	51	100	182
Metastatic serous adenocarcinoma					
Omentum	3 (9)	5 (16)	6 (19)	18 (56)	32
Peritoneum	1 (3)	2 (7)	12 (40)	15 (50)	30
Totals	4	7	18	33	62

Values are represented as n (%). For tumor cells, membranous staining was scored as 0, negative; 1, unable to score; 2, < 60% positive; 3, > 60% positive.